

Analysis of relativistic astrophysical configuration governed by linear equation of state

Kiran Pant,* Pratibha Fuloria

Department of Physics, S.S.J. Campus, Almora, 263601, India

Abstract:

The present paper intends to investigate the behavior of compact relativistic objects consisting of an anisotropic matter distribution with static and spherically symmetric spacetime. Further, an equation of state (EOS) is also considered, which is linear in nature, relating radial pressure and density. As part of this study, various compact stellar models are analyzed based on their physical attributes *CENX – 3*, *4U 1820 – 30*, *PSR1903+327*, *4U1608 – 52*, *PSR1614 – 2230* and *SMCX – 4*. The stellar models presented in this paper are free from singularities and possess all physically plausible features. In order to determine the stability of a compact stellar system, one must consider causality conditions, the adiabatic index, the Buchdhal condition, energy conditions, etc. The presented anisotropic compact stellar model fulfills all these criteria. Moreover, a thorough assessment of all physical properties of the solutions has been conducted for all the compact stars listed above. Based on the analysis of this model conducted analytically and graphically, it is evident that the model is regular and well-behaved. The obtained solution could explain the physics of self-gravitating objects and might be useful in strong-field regimes where data are currently inadequate.

Keywords: General Relativity, Einstein-field equations, Anisotropic fluid distribution, Compact stars, Equation of state.

*e-mail: kiranpant098@gmail.com
e-mail: p.fuloria@yahoo.com

1 Introduction

The study of compact relativistic stars, as well as other gravitational collapse phenomena, has become one of the most challenging aspects of astrophysics [1,2]. In view of this, the modelling of ultra-dense compact celestial entities has been a compelling focal point in relativistic astrophysics for several decades, which are formed by the intense explosions in the universe such as planetary nebulae and supernovas. These structures include neutron stars, white dwarfs, strange stars, hybrid stars, hyperon stars, black holes and gravastars. These compact astrophysical objects provide unique opportunities for studying the properties of matter at extremely dense conditions [3].

Such objects have matter inside at extremely high densities, requiring a different description of stellar plasma than the Newtonian fluid description used in classical physics. Due to their extreme density, such compact objects are relativistic in nature, and therefore, can only be adequately described by Einstein's General Relativity. The strong gravity present in them is one of the most significant factors responsible for a number of fundamental phenomena. Various characteristics of gravitating stars can be attributed to these phenomena. As a matter of fact, useful insights about the development of the cosmos and its constituents are provided by the intricate details of these astronomical objects. Therefore, scientists are highly interested in analyzing their structure and matter composition and put them as a high priority. In physics, the general theory of relativity is a theory that is capable of explaining several phenomena, including a close explanation of the spectral shift of light, perihelion advancement of planets within the solar system, the bending of light due to massive celestial bodies, and several other interesting occurrences. The study of extremely dense relativistic compact stellar objects can be explored and analyzed by the system of Einstein's field equations and imposing conditions for physical acceptability. They provide a more comprehensive understanding of their properties, gravity, matter, and their intricate interactions within the universe. Researchers have been interested in finding the exact solutions to these equations as they have many applications in relativistic astrophysics and serve as a key to unlocking the mysteries of this universe. However, finding their exact solution is an insurmountable challenge [4-6]. Complexities are involved in discovering the exact solutions to Einstein's field equations due to their highly non-linear nature. Despite that, the scientific community is actively engaged in developing several exact solutions to EFE for static and spherically symmetric fluid configurations. The groundbreaking contributions of Schwarzschild [7], Tolman [8], and Oppenheimer and Volkoff [9] deserve special mention in the development of theoretical models for relativistic compact stars. In addition, Chandrasekhar has also made a noteworthy contribution to the modelling of white dwarfs with relativistic corrections [10]. Moreover, Baade and Zwicky introduced the idea of neutron stars as astronomically dense objects resulting from supernova explosions in their pioneering work [11].

A significant contribution was also made by Delgaty and Lake [12] as they successfully formulated various analytical solutions for static spherically symmetric perfect fluid configurations that meet all the required criteria for being physically well-behaved. These compact astrophysical objects can be explored by researchers using different methods and approaches [13-15]. In this context, two methods have been employed. First, a specific form of metric potential is assumed and the equation of state is formulated. This method allows the researcher to explore the relationships between various physical parameters that characterize the compact stellar system. Another avenue involved is to assume an equation of state and solve the field equations to find the remaining physical properties associated with the compact stellar system.

Generally, these compact objects are believed to be made up of a perfect fluid where the radial pressure p_r and the tangential pressure p_t are equal. Nevertheless, there has been substantial empirical evidence suggesting that in highly dense fluids, such as that found within a compact star, the presence of extreme internal density and strong gravity inside the compact stellar system causes an imbalance in the radial and transverse pressure, leading to anisotropy in pressure [16]. The difference between p_t and p_r is known as an anisotropic factor denoted as $\Delta = p_t - p_r$, which could be either positive or negative. The significance of both cases are different. When tangential pressure overpowers radial pressure, it leads to positive anisotropy that results in an outwardly acting force that is repulsive in nature, in opposition to gravitational gradients. Thus the presence of a positive anisotropy factor improves the equilibrium and stability of the system. In contrast, the case of a negative anisotropy factor, where radial pressure is greater than tangential pressure, causes the system to experience an inward or attractive force leading to collapse. Different physical phenomena may contribute to anisotropy. One notable example is the anisotropic distribution of pressure within a neutron star, where the geometric properties of the π = modes contribute to describing a configuration characterized by a condensed phase of pions [17]. In neutron stars, anisotropy may also occur as a result of solids or superfluids inside the core [18]. Anisotropy has also been observed in complex scalar fields that determine self-gravitating objects, as present in boson stars [19-20]. Phase transitions during gravitational collapse [21-22], strong electromagnetic fields [23-25], viscosity [26], slow rotation of a fluid [27] etc. are some of the factors that cause anisotropy. Several authors describe how local anisotropy affects astrophysical objects and their causes [28-33].

A relativistic anisotropic sphere is characterized by several interesting properties that were first discovered by Lemaître [34], in 1933. Nevertheless, Bowers and Liang [35] rekindled the interest in anisotropic compact objects. As a result of these developments, a generalization of the equation of hydrostatic equilibrium was employed to analyze the changes in the surface redshift and gravitational mass. Letelier's contribution in [36] demonstrated that an anisotropic fluid can be generated by the sum of two perfect fluids,

one perfect and the other null. Taking into account the situation in which anisotropic stars exist, two-fluid models of dark matter have been examined in General Relativity [37]. A complete study of all static spherically symmetric anisotropic solutions has been published in [38]. Further, the minimal gravitational decoupling (MGD) technique with different EOS has been extensively employed in the quest for exact solutions for self-gravitating systems, see for instance [39-40]. Furthermore, anisotropy may also have significance in other contexts, such as in exploring the possibility that GW150914 was not caused by a black hole merger but by the merging of rotating gravastars [41-42].

The mass and radius of a compact star constitute its basic characteristics. To address the realistic matter distributions present in stellar structures, a variety of methods and appropriate mathematical assumptions are often employed. In this context, the equation of state (EOS) plays an important role in establishing a mathematical relationship between energy density, pressure and other thermodynamic parameters, thereby linking them to the spacetime curvature, in a manner that is productive and physically plausible. In this way a link is made between such properties and those of nuclear matter and quark matter on a microscopic level through the equation of state (EOS) governing the matter within the star. In the modelling of compact astrophysical entities such as neutron stars and black holes, the interplay between the EOS and general relativity is very crucial [43]. Nuclear interactions in compact stars are relativistic in nature due to the high density of matter inside them. It is important to have a clear understanding of the properties of matter at or near thermodynamic equilibrium to solve many astrophysical problems. As a function of temperature and density, the EOS equation determines the thermodynamic properties such as pressure and entropy of a fluid, that are directly incorporated in the equations used in stellar evolution and determines the mechanical and thermal equilibrium of a star. There are various forms of equations of state, including polytropic, vander waals, chaplygin, quadratic, and linear. Researchers have tried to investigate an EOS that can describe all the large-scale structures and cosmological phenomena due to an inadequate understanding of the exact structure, nuclear interaction, and matter composition of the stars [44-46]. There have been a number of publications describing extra-high density physics using EOS.

In recent years, quark matter has been identified as a component that plays a crucial role in compact star formation, particularly in the core region, where nuclear matter is abundant. The physical processes that determine how quark matter behaves at extremely high densities are still being investigated. Due to this, the astrophysicists have also turned their attention to finding an exact solution to EFEs using LEOS. Several researchers used the linear EOS in solving the field equations and in predicting the behavior of quark matter in an anisotropic domain [47-50]. They have also modeled quark stars in the MIT Bag model by employing a linear EOS. An extensive study has been conducted by Varela et al on the significance of an EOS in stellar models [51]. Based on a particular form of

gravitational potential and isotropic pressure, Komathiraj and Maharaj also found a new class of exact solutions to the Einstein-Maxwell equations [52]. Mak and Harko have also developed a model that explains exactly how an anisotropic quark matter distribution is governed by a linear EOS [53].

Recently, strange stars (SSs) have attracted considerable attention from researchers due to the possibility that compact objects can emit Gravitational Wave Echoes (GWEs). These hypothetical stars possess unique structural and compositional characteristics. It has been discovered that SSs can be ultra-compact stars exhibiting a compactness, sufficient to emit GWE reported in [54-55]. Taking this into account, Bora et al investigate three models of strange star EOSs, the MIT bag model, linear and polytropic models, for a comparative study [56]. They also investigate the possibility of GWE, for these different EOSs. According to this study, not all SSs are capable of emitting GWEs. The emission of GWEs can only be achieved by SSs with the MIT Bag model and linear EOS which meet the criteria for compactness and possess a photon sphere. A star simulation can now be performed using Einstein's field equations, resulting in significant advances in the modelling of star interiors. Researchers have employed a variety of mathematical methods to obtain exact solutions for quark stars based on linear EOS [57- 62]. The research of Patel et al. developed compact star models by incorporating anisotropy into the Finch-Skea spacetime model by employing a generalized EOS [63]. As a result of this equation, they can explore a wide range of physical conditions and provide insight into how matter behaves under extreme gravitational conditions (linear, quadratic, polytropic, Chaplygin, and CFL). The work of Nasheeha focuses on the modelling of anisotropic compact stars using Einstein's field equations based on a generalized equation of state (EOS) and physically reasonable metric potential, allowing models with different types of EOSs to be extracted, including linear, quadratic, polytrope, Chaplygin and color-flavor-locked [64]. In describing compact stars with an anisotropic matter distribution, Sharma and Maharaj developed new solutions for EFEs by assuming a particular mass function. These solutions are distinguished by the fact that they have the potential to be applied to strange stars containing quark matter through the use of linear equations of state [65]. Furthermore, Thirukkanesh and S D Maharaj investigate compact anisotropic stellar models for strange stars consisting quarks under the influence of electromagnetic fields with linear EOS [66]. In addition, they found three classes of new exact solutions to the Einstein Maxwell system by specifying particular forms for gravitational potentials and electric field intensities. Babichev et al. examine the cosmology of a perfect fluid using a linear equation of state to describe both hydrodynamically stable and unstable fluids [67]. A particular feature of the cosmological model considered by them is that it describes the hydrodynamically stable dark energy (and phantom energy). Esculpi proposes two novel sets of compact solutions for a spherically symmetric distribution of matter. These solutions entail an anisotropic fluid sphere endowed with an electrical charge, seamlessly

connected to the Reissner Nordstrom static solution by means of a surface characterized by zero pressure [68]. According to Nilsson et al, Einstein's eld equations are recast as three-dimensional regular ordinary differential equations on a compact state space for static spherically symmetric perfect uid models with a linear barotropic equation of state [69]. Moreover, Pant and Fuloria [70] have published a comparison of linear and quadratic models of dense stellar systems.

Motivated by the above research work, in the present study we have used a particular form of gravitational potential and a linear equation of state to provide new solutions to the eld equations. The entire investigation has been organized into nine sections. In section 2, the necessary physical conditions have been provided that must be met in framing the stellar models. A description of the Einstein eld equations is provided in section 3. A newly proposed solution of anisotropic compact star model is explored in section 4. In Section 5, the matching conditions at the boundary of the interior and exterior spacetime metrics are discussed. There is a discussion of the physical properties, including the central pressure and density values, in section 6. Detailed physical viability and stability of the proposed model is provided in section 7 for all compact stars. In Section 8, we provide a brief summary of the results.

2 Conditions for physical admissibility:

In order to be physically feasible, a compact uid sphere must meet the following conditions:

1. Regularity Conditions: The important requirement for a physically viable stellar structure lies in the well-defined nature of metric potentials at the center. Within compact uid spheres, the metric potentials must be finite and regular without any physical or geometric singularities.
2. Continuity of internal and external metrics: It is essential that both internal and external metrics must be continuous across the boundary of a stellar structure to be physically valid.
3. Equality of radial and transverse pressure at centre of star: Both pressures radial and transverse shares equal values at the centre of stellar structure i. e. i.e. $p_r(0) = p_t(0)$. On approaching the boundary of the star the radial pressure vanishes while transverse pressure persists.
4. Positive and monotonic trends of density and pressures: The physically valid stellar structure necessitates that, inside the stellar structure, both density (ρ) and pressure (p_r, p_t) should be positive and finite, with their maximum values occurring at the center, mathematically represented as i.e. $\rho \geq 0, p_r \geq 0, p_t \geq 0$,

and a monotonically decreasing trend of both on approaching towards the boundary surface of star.

5. Gradients of density and pressure: The gradients of density and pressure must be negative inside the stellar structure, indicating the decrease trend in these parameters towards the stellar boundary, mathematically $\frac{d\rho}{dr} \leq 0$, $\frac{dp_r}{dr} < 0$, $\frac{dp_t}{dr} < 0$.
 6. Anisotropic factor and monotonic variation: The anisotropic factor $\Delta = p_t - p_r$ is also a crucial parameter, mandated to be zero at the centre of star due to equal values of both pressures. On moving towards the boundary the anisotropic factor should monotonically increase, reflecting the evolving balance between radial and transverse pressures within the star.
 7. The profiles of the ratio of stress tensor to energy density $\frac{p_r + 2p_t}{\rho}$ must be less than one and should decreasing in radially outward direction.
 8. Causality conditions: The fulfillment of causality condition must be important. The speed of sound should exhibit a monotonic decreasing function towards the surface. The radial and transverse velocities must be less than the speed of light inside the star, mathematically manifesting as i.e. $0 \leq \frac{dp_r}{d\rho} \leq 1$, $0 \leq \frac{dp_t}{d\rho} \leq 1$.
 9. Both the gravitational and surface redshifts should be positive and finite. There should be a monotonical decrease in gravitational redshift with increasing radius, while the surface redshift should increase as the radius increases and equal to the gravitational redshift at the surface.
 10. Energy conditions: It is necessary to impose some conditions on the linear relationship between energy density and pressure of anisotropic compact stars, which are commonly known as energy conditions. All energy conditions must be met simultaneously by the solution.
 11. Equilibrium condition: In order to achieve equilibrium, the solution must satisfy the TOV equation, also known as the balancing force equation [71-72].
 12. Stability conditions: (a) Herrera (1992) proposed the cracking method to examine the stability of an anisotropic stellar fluid the radial perturbations [73]. Later, by utilizing this cracking concept, Abreu et al. (2007) formulated the stability condition for an anisotropic fluid model. According to this condition, for a compact star $-1 \leq |v_t^2 - v_r^2| \leq 0$ must be satisfied [74].
- (b) Within compact star models, the adiabatic index must be greater than 4/3 for the relativistic isotropic fluid configuration to remain stable.

3 Einstein eld equations

In this study, we intend to develop anisotropic compact stellar models that depict the interior of dense stars. Initially, we start with a line element in curvature coordinates that is static and spherically symmetric. It can be written as follows

$$ds^2 = e^\nu dt^2 - e^\lambda dr^2 - r^2(d\vartheta^2 + \sin^2\vartheta d\phi^2) \quad (1)$$

We can express the energy-momentum tensor of a star assuming that anisotropic matter fills its interior as follows

$$T_{ij} = (\rho + p_\perp)u_i u_j + p_\perp g_{ij} + (p_r - p_\perp)\chi_i \chi_j \quad (2)$$

where ρ, p_r, p_\perp is the matter density, radial pressure, and tangential pressure respectively. u_i, χ_i stands for the four-velocity of the fluid and unit spacelike four-vector directed radially so that $u_i u_i = -1, \chi_i \chi_i = 1$ and $u_i \chi_i = 0$. Einstein's field equations can be derived from spacetime metric (1) and energy-momentum tensor (2) as follows:

$$8\pi\rho = \frac{1 - e^{-\lambda}}{r^2} + \frac{\lambda' e^{-\lambda}}{r} \quad (3)$$

$$8\pi p_r = \frac{e^{-\lambda} \nu'}{r} + \frac{e^{-\lambda} - 1}{r^2} \quad (4)$$

$$8\pi p_t = \frac{e^{-\lambda}}{4} [2\nu'' + \nu'^2 - \nu' \lambda' + \frac{2\nu'}{r} - \frac{2\lambda'}{r}] \quad (5)$$

The anisotropic factor can be defined by making use of Eqs. (4-5) as follows

$$8\pi\Delta(r) = 8\pi(p_r - p_\perp) = \frac{e^{-\lambda}}{4} [2\nu'' + \nu'^2 - \nu' \lambda' - \frac{2(\lambda' + \nu')}{r}] + 4 \frac{e^{-\lambda} - 1}{r^2} \quad (6)$$

A prime (') represent a differentiation with respect to r . The system of equations from (3-5) determines how an anisotropic fluid distribution behaves in the gravitational field.

4 New Generated physically viable Model

As a first step toward developing a physically plausible representation of the stellar system, it is assumed that the metric potential g_{rr} is expressed as follows:

$$e^\lambda = 1 + ar^2 + br^4 \quad (7)$$

Where, two constant parameters, a and b , whose units are km^{-2} and km^{-4} respectively, determined from the matching conditions. Earlier, Tolman [75] proposed this metric potential, which was later adopted by Biswas et al. [76] for modelling realistic compact stellar objects. In the past, several authors have used this ansatz to model compact stars [77-78]. This ansatz is characterized by being free from the central singularity and having a monotonous increase with r . Equation (7) and (3) leads to,

$$\rho = \frac{1 - (1 + ar^2 + br^4)^{-1}}{r^2} + \frac{(2ar + 4br^3)(1 + ar^2 + br^4)^{-2}}{r} \quad (8)$$

The density $\rho(r)$ represented in the above expression is finite at the centre of the star. Since the EOS provides the valuable information about the properties of different mixtures of liquids, substances, and other constituents of matter inside a star. Hence many researchers have presented a lot of research ideas on the linear equation of state. Our model considers an EOS whose density ρ and pressure p_r are linearly related as follows

$$p_r = A\rho - B, \quad (9)$$

where, A and B represents the constants. The following condition is used to determine the radius of the star

$$p_r(r = R) = 0, \quad (10)$$

yielding,

$$B = A\rho_a \quad (11)$$

On Substituting the Eq. (11) into 9), it gives

$$P_r = A\rho - A\rho_a = A(\rho - \rho_a). \quad (12)$$

From Eqs. (12) and (5), the obtained expression for ν' is given as follows

$$\nu' = re^\lambda [A(\rho - \rho_a) - \frac{e^{-\lambda} - 1}{r^2}] \quad (13)$$

$$\nu' = A [2ar + br^3 + \frac{2ar + 4br^3}{1 + ar^2 + br^4} - 3ar(1 + ar^2 + br^4)] \quad (14)$$

$$v'' = a + 3br^2 + A \left[\frac{(2a+12br^2)(1+ar^2+br^4) - (2ar+4br^3)^2}{(1+ar^2+br^4)^2} \right] \quad (15)$$

$$v = \frac{C + A \log(1 + ar^2 + br^4) + (1 + A) \left(\frac{ar^2}{2} + \frac{br^4}{4} \right) - \alpha \left(\frac{3Ar^2}{2} + \frac{3Aar^2}{4} + \frac{Abr^6}{2} \right)}{1} \quad (16)$$

where, C is integration constant. Making use of the Eqs. (4-5) we can also obtain the expressions for p_r , p_t as follows

$$p_r = \frac{2A(3a + (a^2 + 5b)r^2 + 2abr^4 + b^2r^6) - 3A\alpha (ar^2 + br^4 + 1) (a + 2br^4 + 2)}{16\pi (ar^2 + br^4 + 1)^2} \quad (17)$$

$$p_t = \frac{-4r^4(a + 2br^2 + 2 - 2br^4) + (A + 1)r(a + br^2) + \frac{2Ar(a + 2br^2)}{ar^2 + br^4 + 1} - \frac{3}{2}\alpha Ar(a + 2 + 2br^4) + (r + ar^3 + br^5) + (A + 1)r(a + br^2) + \frac{2Ar(a + 2br^2)}{ar^2 + br^4 + 1} - \frac{3}{2}\alpha Ar(a + 2br^4 + 2) + 2r(1 + ar^2 + br^4) - \frac{4A(ar + 2br^3)^2}{(ar^2 + br^4 + 1)^2} + \frac{2A(a + 6br^2)}{ar^2 + br^4 + 1} - \frac{3}{2}\alpha A(a + 10br^4 + 2)}{32\pi r (ar^2 + br^4 + 1)^2} \quad (18)$$

$$\Delta = \frac{\begin{aligned} & -2(1 + 2ar^2 + 3br^4) \left[\frac{2Ar(a + 2br^2)}{ar^2 + br^4 + 1} - \frac{3}{2}\alpha Ar \right] (a + 2br^4 + 2) \\ & + (r + ar^3 + br^5) \left[\frac{2Ar(a + 2br^2)}{ar^2 + br^4 + 1} - \frac{3}{2}\alpha Ar \right] (a + 2br^4 + 2) \\ & + (1 + A)r(a + br^2) \\ & + 2r(1 + ar^2 + br^4) \left[\frac{2A(a + 6br^2)}{ar^2 + br^4 + 1} - \frac{3}{2}\alpha A \right] (a + 10br^4 + 2) \\ & - \frac{4A(ar + 2br^3)^2}{(ar^2 + br^4 + 1)^2} \end{aligned}}{32\pi r (ar^2 + br^4 + 1)^2} \quad (19)$$

5 Boundary Condition

At the boundary of stellar configuration, we should match smoothly the metric of interior spacetime with the schwarzschild exterior spacetime

$$ds^2 = \left(1 - \frac{2m}{r}\right) dt^2 - \left(1 - \frac{2m}{r}\right)^{-1} dr^2 - r^2 d\Omega^2 \quad (20)$$

Where, $d\Omega^2 = (d\vartheta^2 + \sin^2\vartheta d\varphi^2)$, and $M = m(R)$ represents the total mass at boundary R . When the metric functions are continuous at the boundary ($r = R$), we obtain the following result

$$e^{-\lambda}_{r=R} = \left(1 - \frac{2m}{r}\right) \quad (21)$$

$$e^{\nu}_{r=R} = \left(1 - \frac{2m}{r}\right) \quad (22)$$

Another necessary condition is

$$p_{r(r=R)} = 0 \quad (23)$$

Taking into account the continuity for both metric matching $e^{-\lambda}_{r=R} = e^{\nu}_{r=R}$, the following constants can be determined:

$$a = \frac{2M(1 + bR^4) - bR^5}{r^2(R - 2M)} \quad (24)$$

$$C = \frac{\left[\log \left(1 - \frac{2m}{r} \right) + \alpha \left(\frac{3Ar^2}{2} + \frac{3Aar^2}{4} + \frac{Abr^6}{2} \right) \right]}{A \log(1 + ar^2 + br^4) - (1 + A) \left(\frac{ar^2}{2} + \frac{br^4}{4} \right)} \quad (25)$$

Also, the necessary condition $p_{r(r=R)} = 0$, at the boundary yields

$$\rho - \frac{3\alpha}{8\pi} = 0 \quad (26)$$

$$\alpha = \frac{8\pi\rho}{3} \quad (27)$$

As ρ is positive, α is also positive.

6 Prerequisites for a solution to be well-behaved

There are several conditions that has been checked before to validate the constructed stellar models. These conditions have been checked for the stars *CENX – 3*, *4U 1820 – 30*, *PSR1903 + 327*, *4U1608 – 52*, *PSR1614 – 2230* and *SMCX – 4*.

6.1 Regularity Conditions of metric potentials:

The important features regarding the metric potentials $e_\lambda(r) \geq 0$, $e_\nu(r) \geq 0$, $0 \leq r \leq a$. are demonstrated in Fig.(1a) and Fig.(1b). As a result, we are able to select parameters that are appropriate for our model based on the conditions described above. The Eqs. (7) and (16), shows that $e^\lambda(0) = 1$ and $e^\nu(0) = \text{constant}$. In addition, both the derivatives of the metric functions at the center are zero. Thus, from these features one can conclude that the metric functions of both type are showing regular and well behaved pattern inside the stellar structure.

6.2 Trends of density and anisotropy:

The graphical patterns of density and anisotropy are shown in Figs. (2a) and (2b), portraying the well behaved patterns of all these physical quantities.

6.3 Monotonic decrease of pressures:

The trends of pressures (radial and transverse) are illustrated in Figs.(3a) and (3b), depicting that inside the stellar con guration they both are nite and positive at the

centre. As one moves towards the boundary, p_r is zero, while p_t is not.

6.4 Trends of Gradients

Realistic stellar models should exhibit the following characteristics $\frac{dp}{dr} \leq 0$, $\frac{dp_r}{dr} \leq 0$, $\frac{dp_t}{dr} \leq 0$ for $0 \leq r \leq R$. All of these requirements are met by the current proposed model depicted in Figs.(4a, 4b and 4c). Furthermore, the well-behaved nature of the stress tensor has been portrayed in Fig.(4d).

6.5 Equation of states

There is also a need to discover a relationship between pressure and density, known as equation of state. The well behaved nature of equation of states throughout the stellar structure are also depicted in Figs. (5a) and (5b), validating the physical viability of proposed model.

6.6 Energy Condition:

The following inequalities must be simultaneously satisfied at every point within an anisotropic uid sphere to constitute a physically acceptable matter composition. Figs. (6b, 6c, 6d and 6a) shows that each of the energy conditions, namely Null Energy Condition (NEC), Weak Energy Condition (WEC), Dominant Energy Condition (DEC), Strong Energy Condition (SEC), and Trace Energy Condition (TEC) respectively, all are satisfied by our model.

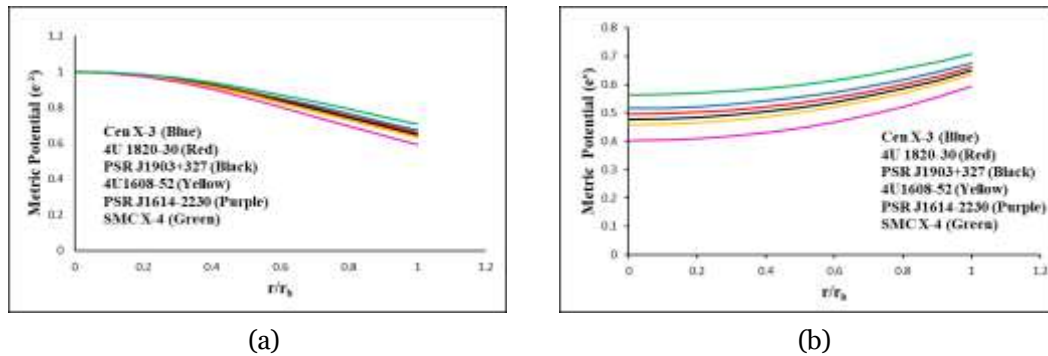


Figure 1: (a) Outmarch of metric potentials $e^{-\lambda}$, and (b) e^{ν} , against fractional radial coordinate r/r_b

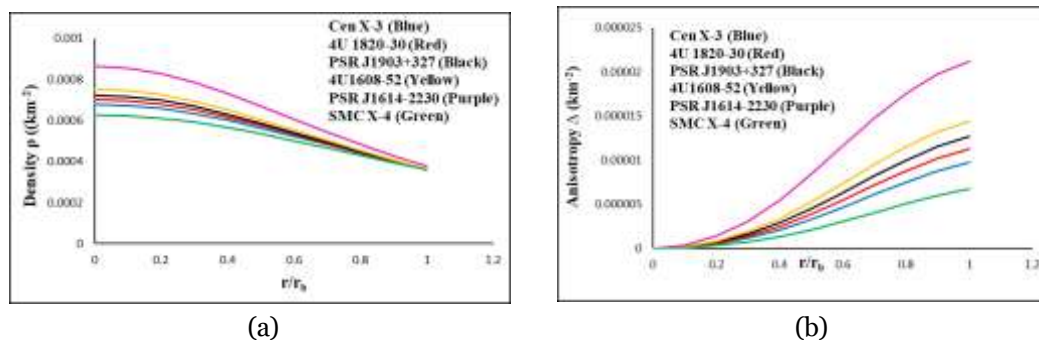


Figure 2: (a) Outmarch of density ρ , and (b) anisotropy (Δ), against fractional radial coordinate r/r_b

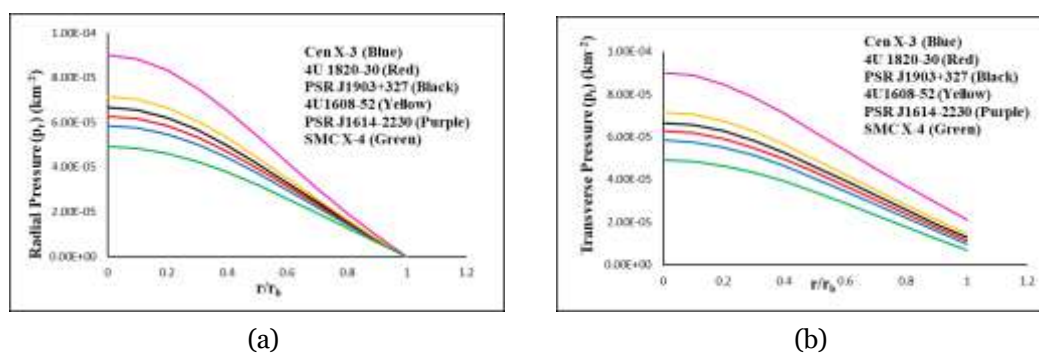


Figure 3: (a) Outmarch of radial pressure p_r , and (b) transverse pressure p_t , against fractional radial coordinate r/r_b

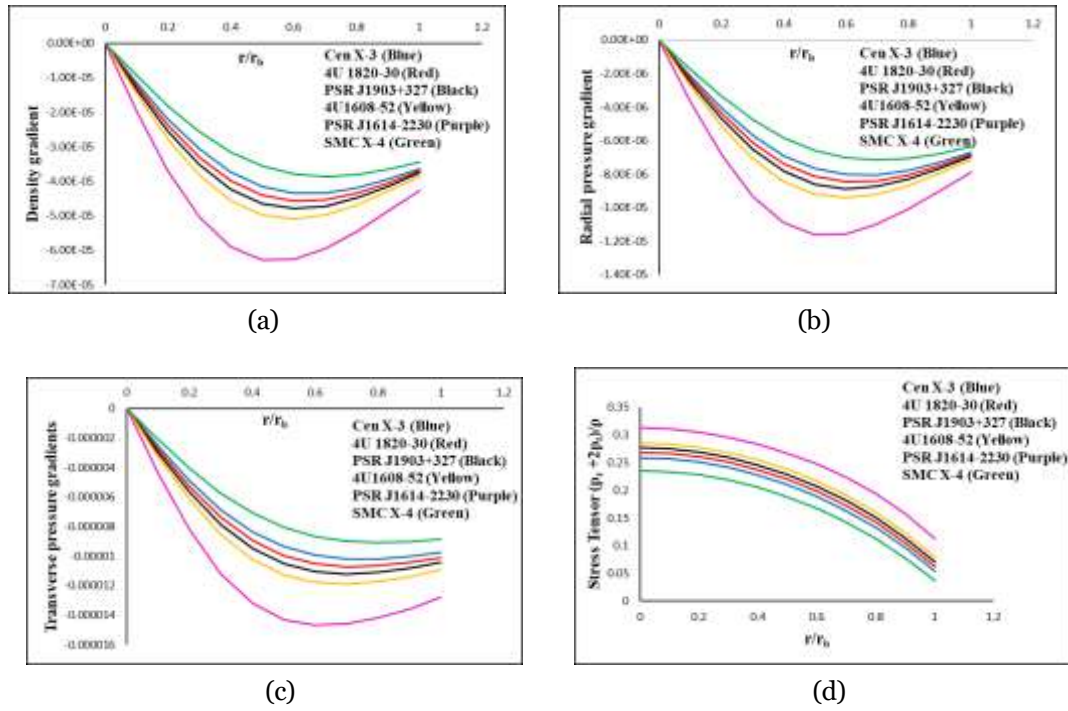


Figure 4: Plots of, (a) Density gradient $\frac{d\rho}{dr}$, (b) Radial pressure gradient $\frac{dp_r}{dr}$, (c) Transverse pressure gradient $\frac{dp_t}{dr}$, (d) Stress tensor, with fractional radial coordinate r/r_b

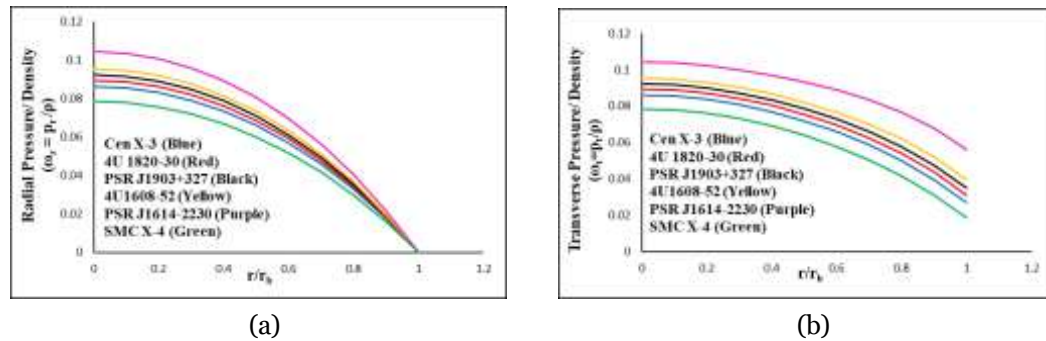


Figure 5: Plots of, (a) equation of state $\omega_r(r)$, and (b) $\omega_t(r)$, with radial coordinate r/r_b

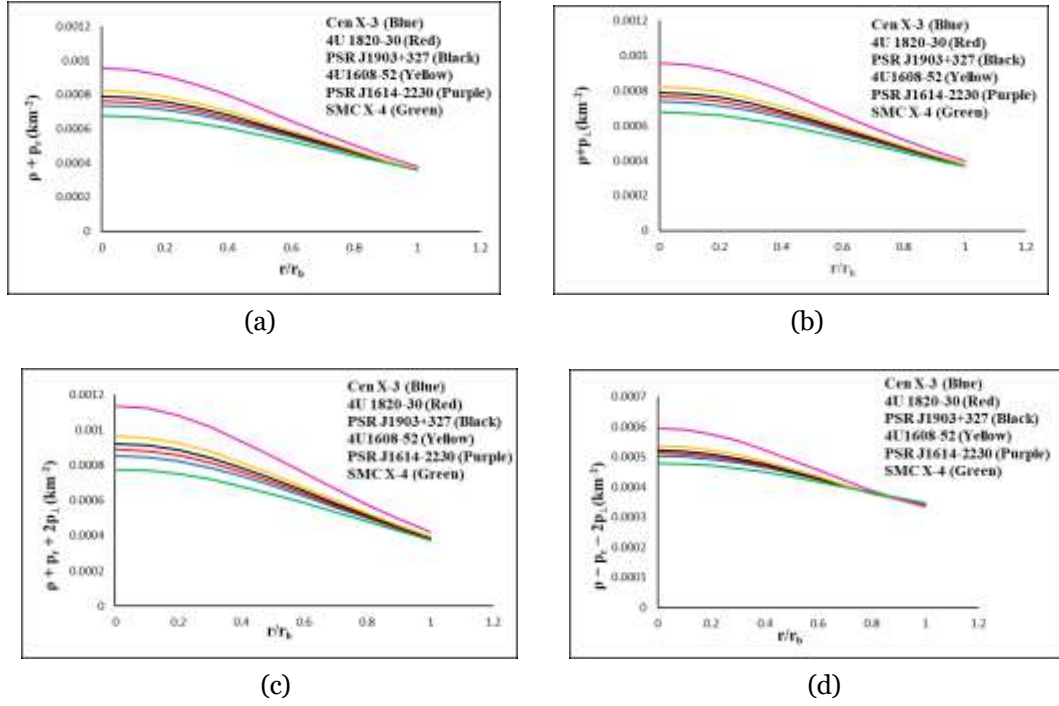


Figure 6: Trends of different energy conditions with fractional radial coordinate r/r_b

- (i) NEC : $\rho + p_r \geq 0, \rho + p_\perp \geq 0,$
- (ii) WEC : $\rho + p_r > 0, \rho > 0,$
- (iii) DEC : $\rho > |p_r|, \rho > |p_\perp|,$
- (iv) SEC : $\rho + p_r + 2p_\perp \geq 0,$
- (v) T EC : $\rho - p_r - 2p_\perp \geq 0.$

6.7 Monotony Condition

6.8 Mass radius relationship and compactness factor

Since the mass function $m(r)$ is connected to the metric potential by the relation $e^{-\lambda} = 1 - \frac{2m}{r}$, Based on this, the mass function can be obtained as follows:

$$m(r) = 4\pi \int_0^r r^2 \rho(r) dr = \frac{1}{2} r - \frac{r}{(1 + ar^2 + br^4)} \quad (28)$$

$$u(r) = \frac{m(r)}{r} = \frac{1}{2} - \frac{2}{2(1 + ar^2 + br^4)} \quad (29)$$

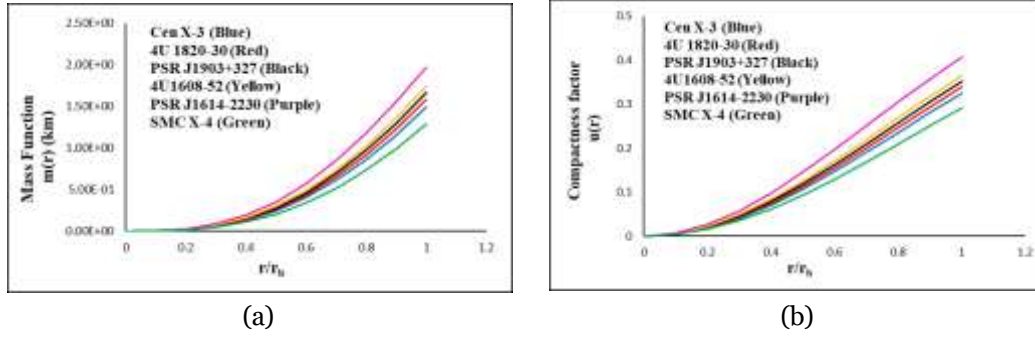


Figure 7: Plots of, (a) mass function $m(r)$, and (b) compactness factor $u(r)$, with radial coordinate r/r_b

Figs. (7a) and (7b) illustrates the graphical profiles of mass function and compactness respectively. There is a monotonic increase in both these functions with respect to r/r_b

6.9 Causality Condition:

$$v_r = \frac{S}{\frac{dp_r}{dp}} = \sqrt{A} \quad (30)$$

$$v_t = \frac{S}{\frac{dp_t}{dp}} \quad (31)$$

Inside the stellar configuration, the causality condition requires that $0 \leq \frac{dp_r}{dp} \leq 1$ and $0 \leq \frac{dp_t}{dp} \leq 1$. The sound speed must be between 0 and 1. Also Eq.(9) shows that $\frac{dp_r}{dp}(r=0) = A$. From the table 1, $0 \leq A \leq 1$. All features are satisfied by the proposed model as shown in their graphical profiles Figs. (8a) and (8b).

7 Physical Viability and Stability

7.1 Herrera condition for stability

Herrera's cracking concept [71] can also be used to assess the stability of anisotropic stellar models. It is proposed that the "no cracking" concept is crucial for the potentially stable region $|\nu_t^2 - \nu_r^2| \leq 1$ in order to achieve a stable configuration. To validate our model, this

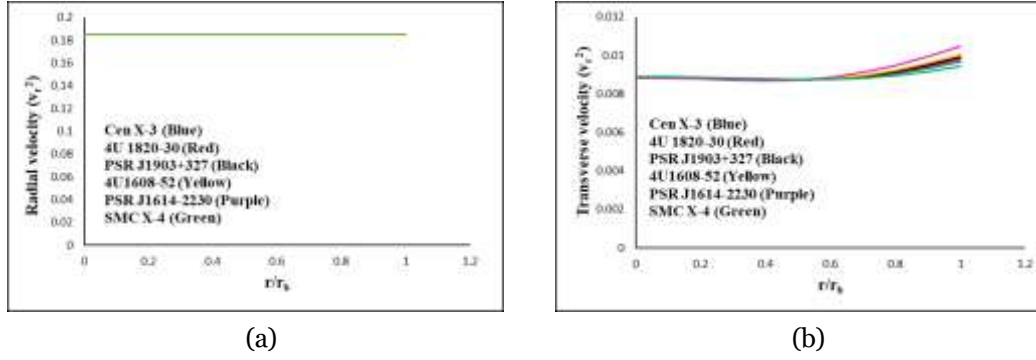


Figure 8: Outmarch of, (a) Radial velocity, (b) transverse velocity, with the fractional radial coordinate r/r_b .

condition is extended by Abreu et al. [72], to analyze potentially stable regions within the stellar con guration as follows:

$$-1 \leq v_t^2 - v_r^2 \leq 0 \Rightarrow \text{Potentially Stable,}$$

$$0 \leq v_t^2 - v_r^2 \leq 1 \Rightarrow \text{Potentially Unstable,}$$

As can be seen from the plots in Fig. (9a), the di erence between square of sound speeds falls within the range of -1 and 0 . Therefore, it is apparent that our model meets the stability criteria.

7.2 Adiabatic index for stability

In a relativistic anisotropic stellar con guration, the adiabatic index de nes the stability of the system represented as

$$\Gamma = \frac{\rho + p_r}{p_r} \frac{dp_r}{dp} \quad (32)$$

Any stellar con guration will remain stable if the adiabatic index is greater than $4/3$, which physically characterises the sti ness of the EOS for a given density. Moreover, the pro le of the adiabatic index shown in Fig.(9b) inside the stellar interior is monotonically increasing and surpassing $4/3$ everywhere.

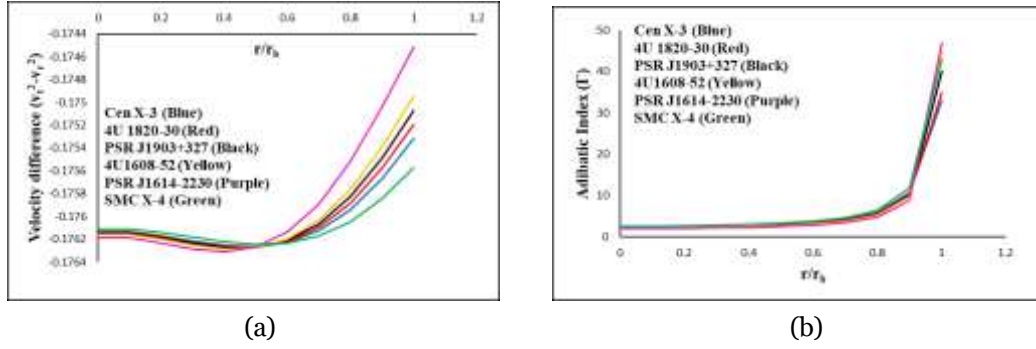


Figure 9: Graphical Profiles of, (a) square of velocity difference, (b) adiabatic index, with the fractional radial coordinate r/r_b

7.3 Stability under three different forces

There are three forces that influence a star in order to maintain static equilibrium: hydrostatic force (F_h), and anisotropic force (F_a), gravitational force (F_g). Fig. (10a,10b) illustrates the conservation equation that is described by the Tolman-Oppenheimer-Volkoff (TOV) equation

$$\nabla^\mu T_{\mu\nu} = 0 \quad (33)$$

Utilizing the Eq. (2) into (33) the following equation can be obtained:

$$-\frac{v'}{2}(\rho + p_r) + \frac{2}{r}(p_t - p_r) = \frac{dp_r}{dr} \quad (34)$$

The above equation may also be expressed as

$$F_g + F_a + F_h = 0, \quad (35)$$

$$\text{where, } F_g = -\frac{v'}{2}(\rho + p_r), F_a = \frac{2}{r}(p_t - p_r) \text{ and } F_h = -\frac{dp_r}{dr} \quad (36)$$

$$F_g(r) = - \frac{3\alpha A (ar^2 + br^4 + 1) (a + 2br^4 + 2) - 2(A + 1) r^2 (a^2 + 5b + 2abr^4 + 3a + b^2r^6) - 2r^3(a^2(A + 1) + 5Ab + b) - 4a(A + 1)br^5}{16\pi (ar^2 + br^4 + 1)^3} \quad (37)$$

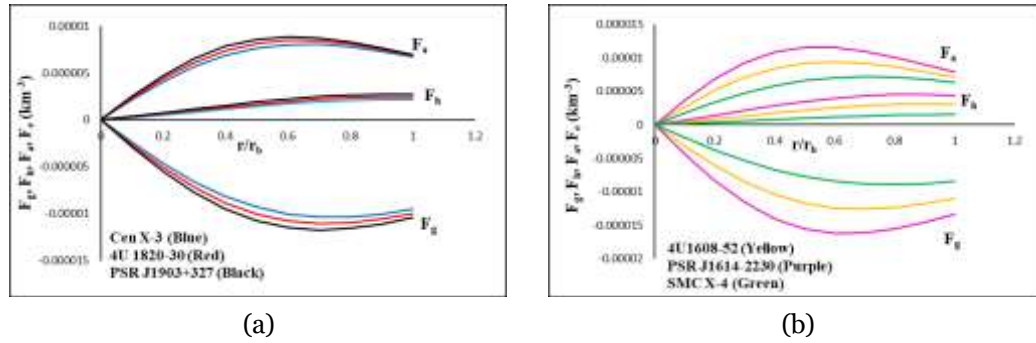


Figure 10: Plots of different forces F_a, F_h, F_g , (a) For stars *CenX* – 3, *4U*1820 – 30, and *PSR*J1903 + 327, (b) For stars *4U*1608 – 52, *PSR*J1614 – 2230, and *SMC*X – 4, with radial coordinate r/r_b .

$$F_h(r) = \frac{\left\{ \frac{2}{3} \frac{3br^4}{a^2 + 4b} + \frac{ar^2}{a^2 + 13b} + \frac{5a^2 + 3ab^2r^6 + b^3r^8 - 5b}{a^2 + 13b} \right\}^{\#} - 3\alpha \frac{ar^2 + br^4 + 1}{r^2 + 2}}{8\pi (ar^2 + br^4 + 1)^3} \quad (38)$$

$$F_a(r) = \frac{\begin{aligned} & -4r(a + 2br^2) - 4Ar(3a + (a^2 + 5b)r^2 + 2abr^4 + b^2r^6) \\ & + 6\alpha Ar \frac{ar^2 + br^4 + 1}{a + 2br^2 + 2} + \frac{2Ar}{a + br^2} \frac{a + 2br^2}{ar^2 + br^4 + 1} \\ & + (2 - 2br^4) \left[\frac{A+1}{A+1} r \frac{a + br^2}{a + 2br^4 + 2} - \frac{3}{2} \alpha Ar \frac{a + 2br^4 + 2}{a + br^2} \right. \\ & \left. + (r + ar^3 + br^5) \left[\frac{A+1}{A+1} r \frac{a + br^2}{a + 2br^4 + 2} - \frac{3}{2} \alpha Ar \frac{a + 2br^4 + 2}{a + br^2} \right] \right. \\ & \left. - \frac{4A}{(ar^2 + br^4 + 1)^2} \frac{ar + 2br^3}{(ar^2 + br^4 + 1)^2} \right] \\ & + \frac{2A}{ar^2 + br^4 + 1} \frac{a + 6br^2}{a + 10br^4 + 2} - \frac{3}{2} \alpha A \frac{a + 10br^4 + 2}{a + 10br^4 + 2} \end{aligned}}{16\pi (ar^2 + br^4 + 1)^3} \quad (39)$$

The Figs.(10a and 10b) shows that the system is maintained in static equilibrium by hydrostatics and anisotropic force being positive, while gravitation is negative.

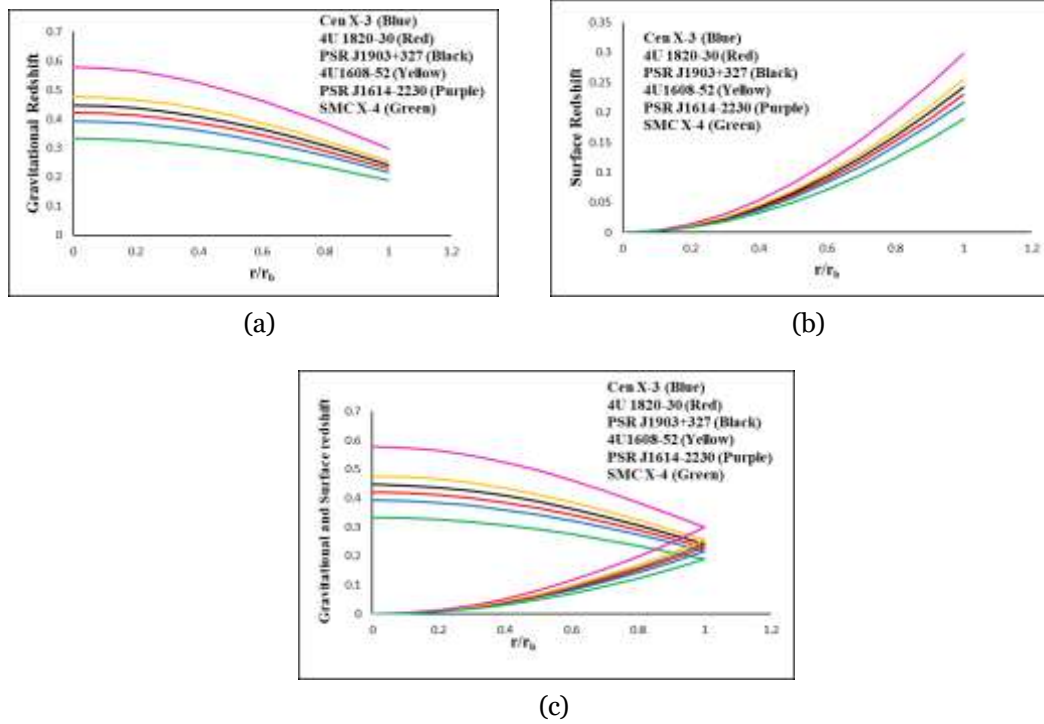


Figure 11: Plots of, (a) gravitational redshift, (b) surface redshift, (c) both redshifts combined, with radial coordinate r/r_b

7.4 Gravitational Redshift and Surface Redshift

The surface redshift z_s of the stellar con guration can be obtained as follows

$$z_s = \left(1 - \frac{2m}{r}\right)^{-1} - 1 = -1 + \sqrt{\frac{1}{1 + ar^2 + br^4}} \quad (40)$$

The gravitational redshift of the stellar con guration

$$z_g = e^{-\nu/2} - 1 \quad (41)$$

Figs.(11a) and (11b) show the profiles of gravitational and surface redshift as a function of r/r_b . Fig.(11a) shows the profile of gravitational redshift in relation to r , indicating a monotonous decrease in the redshift, while the surface redshift in Fig.(11b) monotonically increases with the increase of fractional coordinate " r/r_b ". A combination of both gravitational and surface redshifts are shown in Fig. 11c. The concept of surface redshift is useful in explaining how an equation of state of stars is influenced by its internal particles. Our model predicts a stable compact star based on a profile of gravitational

Table 1: Numerical values of different physical parameters entails in the present study of different compact stars *CENX – 3*, *4U 1820–30*, *PSR1903+327*, *4U 1608–52*, *PSRJ1614 – 2230* and *SMCX – 4*

S. No.	Name of Star	A	$b(km^{-4})$	$a(km^{-2})$	α	C
1	CEN X-3	0.185	0.00000045	0.003038861	0.003038861	-0.661989865
2	4U 1820-30	0.185	0.00000045	0.003035943	0.003035943	-0.702167003
3	PSR 1903+327	0.185	0.00000045	0.003034214	0.003034214	-0.738780706
4	4U1608-52	0.185	0.00000045	0.00305457	0.00305457	-0.779277188
5	PSR J1614-2230	0.185	0.00000045	0.003166455	0.003166455	-0.912433613
6	SMC X-4	0.185	0.00000045	0.003028275	0.003028275	-0.574093333

redshift and surface redshift.

Table 2: Comparison of observational values and calculated values of masses and radii for the compact stars *CENX – 3*, *4U 1820 – 30*, *PSR1903 + 327*, *4U 1608 – 52*, *PSRJ1614 – 2230* and *SMCX – 4*

S. No.	Name of Star	Observed value $M(M_o)$		Observed value R (km)		Calculated $M(M_o)$	Calculated $R(km)$
1	CEN X-3	1.49	0.08	9.178	0.13	1.49	9.17000
2	4U 1820-30	1.58	0.06	9.316	0.086	1.58	9.31599
3	PSR 1903+327	1.667	0.021	9.438	0.03	1.66	9.43799
4	4U1608-52	1.74	0.14	9.528	0.15	1.74	9.52799
5	PSR J1614-2230	1.97	0.04	9.69	0.2	1.97	9.69000
6	SMC X-4	1.29	0.05	8.831	0.09	1.29	8.83100

Table 3: Calculated values of Central density, central pressure, compactness parameter and surface redshift for the compact stars *CENX* – 3, *4U* 1820 – 30, *PSR*1903 + 327, *4U*1608 – 52, *PSR*J1614 – 2230 and *SMCX* – 4

S. No.	Name of Star	$\rho_c(\text{gm/cm}^3)$	$p_c(\text{dyne/cm}^2)$	$u = 2M/R$	z_s
1 15	CEN X-3	$0.9154314 * 10$	$7.09722 * 10^{34}$	0.324972737	0.217136659
2 15	4U 1820-30	$0.9457380 * 10$	$7.60961 * 10^{34}$	0.339201374	0.230170857
3 15	PSR 1903+327	$0.9741371 * 10$	$8.08707 * 10^{34}$	0.351769443	0.242039049
4 15	4U1608-52	$1.0136183 * 10$	$8.68981 * 10^{34}$	0.365239295	0.255148129
5 15	PSR J1614-2230	$1.1678239 * 10$	$10.9573 * 10^{34}$	0.406604747	0.298159232
6 15	SMC X-4	$0.8462128 * 10$	$5.97320 * 10^{34}$	0.292152644	0.188584857

8 Discussion and conclusions:

Using an anisotropic material distribution and a physically plausible metric potential, we obtain a new well-behaved solution of the Einstein field equation for spherically symmetric fluid spheres. The present study involves the development of compact stellar models for six stars, including *CENX* – 3, *4U* 1820 – 30, *PSR*1903 + 327, *4U* 1608 – 52, *PSR*J1614 – 2230 and *SMCX* – 4. Several constants (A, b, a, α, C) associated with the present solution have been determined via the boundary conditions in which the interior line element must be compared with the exterior Schwarzschild line element at the stellar boundary. By plugging the values of these constants into expressions, we portrayed a variety of physical variables graphically. In table 1 we have presented the values of all these constant parameters (A, b, a, α, C) for all six stellar candidates *CENX* –3, *4U* 1820–30, *PSR*1903+327, *4U* 1608–52, *PSR*J1614–2230 and *SMCX* –4.

The graphical representation of the profiles of the metric potentials are depicted in Figs. (1a) and (1b), that increases as we move from the center towards the boundary with the radial coordinate (r). The graphical profiles of physical parameters, namely matter density (ρ), radial and transverse pressure (p_r, p_t) are provided in the Figs. (2a), (3a) and (3b) respectively. At the center, these parameters have positive definite values, and as they move towards the boundary, they decrease monotonically. When the boundary is reached, the radial pressure falls to zero, but the transverse pressure and matter density remain non-zero values. These variables are decreasing in nature, which provides a strong foundation for the stability of our models. According to Fig (2b), the anisotropic

factor increases from the center toward the boundary when moving away from the center. According to the positive anisotropy, the transverse pressure p_t prevails over the radial pressure p_r , demonstrating that the force is repulsive in nature and that the compact structure is anisotropic. It can also be seen from figure that the anisotropy disappears at the central point of the model, which is a necessary condition for a structure to be physically acceptable. The Figs. (4a, 4b and 4c) represents that there are negative values for density gradients, radial pressure gradients, and transverse pressure respectively. There are negative gradients within the stellar structures, which confirm the decreasing trends in density and pressure. From Fig (4d) we observe that the ratio of the trace of stress tensor to the energy density remains below one and a monotonic decrease is observed from the center of the star to its boundary.

In Figs. (7a, 7b), we examine the variation of the compactness factor and mass function with respect to radial coordinates r . The compactification factor of compact stars increases with distance from their centers to their surfaces and is estimated to fall within the Buchdahl limit ($u < \frac{4}{9}$). A graphic representation of the four energy conditions are provided in Figs. (6a, 6b, 6c and 6d), illustrating the null energy condition (NEC), the weak energy condition (WEC) and the strong energy condition (SEC), trace energy condition (TEC) respectively for our model. Based on the graph in Fig. (11a), it is apparent that gravitational redshift decreases while surface redshift displayed in Fig. (11b) is positive, finite, and monotonically increasing with increasing radial coordinates. From the graph (8a, 8b), it is clear that both radial and transverse velocities are less than unity ($0 < \frac{dp_r}{dp} < 1$ and $0 < \frac{dp_\perp}{dp} < 1$) within stellar structures, confirming that our model follows the causality condition. The inequality of Herrera's cracking concept $-1 \leq v_t^2 - v_r^2 \leq 0$ is an essential requirement for determining the stability of an anisotropic object, which is fully satisfied by *CENX* – 3, *4U* 1820 – 30, *PSR*1903 + 327, *4U* 1608 – 52, *PSR*J1614 – 2230 and *SMCX* – 4 as portrayed in Figs. (9a). In Fig. (9b), the adiabatic index profile can be seen. From the figure, it is clear that the adiabatic index is $\Gamma_r = \frac{\rho + p_r}{p_r} \frac{dp_r}{dp} > \frac{4}{3}$ throughout the stellar structure, and therefore this model is stable and non-collapsing. Fig. (10a) and Fig. (10b) illustrate the different types of forces. It can be seen from the figures, the dominant gravitational force (F_g) is counterbalanced by the simultaneous actions of anisotropic and hydrostatic forces (F_a and F_h).

The results demonstrate that all thermodynamic variables and geometrical variables exhibit well behaved patterns, validating the stability criteria for *CENX* – 3, *4U* 1820 – 30, *PSR*1903 + 327, *4U* 1608 – 52, *PSR*J1614 – 2230 and *SMCX* – 4. The models can therefore be considered to be physically acceptable structures. We have also calculated the mass and radius of all six stars, as shown in table 2, by using the constants α , β , γ listed in Table 1 and the boundary condition $p_r(r = R) = 0$. The computed masses and radii of the compact stellar models *CENX* – 3, *4U* 1820 – 30, *PSR*1903 + 327, *4U* 1608 – 52, *PSR*J1614–2230 and *SMCX* –4 appears to be very close to those of Gangopadhyay et al. [79]. Moreover, for all these compact stellar objects, table 3 provides calculations for

the central density, central pressure, compactness factor, and surface redshift. Based on the results of this study, these models have the potential to have significant astrophysical implications especially for scientists involved in this field of research.

References

- [1] S. L. Shapiro and S. A. Teukolsky, Black holes, white dwarfs, and neutron stars: The physics of compact objects, New York, USA: Wiley (1983) 645 p.
- [2] D. Psaltis, Living Rev. Rel. 11 (2008) 9 [arXiv:0806.1531 [astro-ph]].
- [3] D. R. Lorimer, Living Rev. Rel. 11 (2008) 8 [arXiv:0811.0762 [astro-ph]].
- [4] P. K. Kuh tting, Some remarks on exact wormhole solutions, Advanced Studies in Theoretical Physics, 5 (2011) 365-367.
- [5] J. Bicak, Einstein equations: exact solutions, Encyclopedia of Mathematical Physics, 2 (2006) 165-173.
- [6] M. Malaver, Black Holes, Wormholes and Dark Energy Stars in General Relativity, Lambert Academic Publishing, Berlin, (2013).
- [7] K. Schwarzschild, Uber das Gravitations Feld einer Kugel aus inkompressibler Flus-
sigkeit nach der Einsteinschen Theorie, Math. Phys. Tech., 23 (1916) 424-434.
- [8] R. C. Tolman, Static solutions of Einstein's eld equations for spheres of uid, Phys-
ical Review, 55 (4) (1939) 364-373.
- [9] J. R. Oppenheimer and G. Volko , On massive neutron cores, Physical Review, 55
(4) (1939) 374-381.
- [10] S. Chandrasekahr, The maximum mass of ideal white dwarfs, Astrophysical Journal,
74 (1931) 81-82.
- [11] W. Baade and F. Zwicky, On Super-novae, Proceedings of the National Academy of
Sciences of the United States of America, 20 (5) (1934) 254-259.
- [12]] M. S. R. Delgaty and K. Lake, Physical Acceptability of Isolated, Static, Spheri-
cally Symmetric, Perfect Fluid Solutions of Einstein's Equations, Computer Physics
Communications, 115 (1998) 395-415.
- [13] Malaver, M. (2013). Black Holes, Wormholes and Dark Energy Stars in General
Relativity. Lambert Academic Publishing, Berlin. ISBN: 978-3-659-34784-9.
- [14] Komathiraj K., and Maharaj S.D. (2008). Classes of exact Einstein-Maxwell solu-
tions, Gen. Rel. Grav. 39, 2079-2093.

- [15] Sharma, R., Mukherjee, S and Maharaj, S.D. (2001). General solution for a class of static charged stars, *Gen. Rel. Grav.* 33, 999-110.
- [16] M. Ruderman, Pulsars: Structure and dynamics, *Annu. Rev. Astron. Astrophys.* 10, (1972) 427.
- [17] F. Sawyer and D. J. Scalapino, Pion condensation in superdense nuclear matter, *Phys. Rev. D* 7, (1973) 953.
- [18] H. Heiselberg and M. H. Jensen, Phases of dense matter in neutron stars, *Phys. Rep.* 328, (2000) 237.
- [19] M. Gleiser, Stability of boson stars, *Phys. Rev. D* 38, (1988) 2376.
- [20] M. Gleiser, Gravitational stability of scalar matter, *Nucl. Phys. B* 319, (1989) 733.
- [21] Sokolov, A.: Phase transformations in a super uid neutron liquid. *Zhurnal Eksperimental'noj i Teoreticheskoy Fiziki* 49(4), 1137 1140 (1980)
- [22] Herrera, L., Nunez, L.: modelling 'hydrodynamic phase transitions' in a radiating spherically symmetric distribution of matter. *The Astrophysical Journal* 339, 339 353 (1989)
- [23] Weber, F.: Quark matter in neutron stars. *Journal of Physics G: Nuclear and Particle Physics* 25(9), 195 (1999)
- [24] Martinez, A.P., Rojas, H.P., Cuesta, H.M.: Magnetic collapse of a neutron gas: Can magnetars indeed be formed? *The European Physical Journal C-Particles and Fields* 29, 111 123 (2003)
- [25] Usov, V.V.: Electric elds at the quark surface of strange stars in the color-avor locked phase. *Physical review D* 70(6), 067301 (2004) .
- [26] Ivanov, B.: The importance of anisotropy for relativistic uids with spherical symmetry. *International Journal of Theoretical Physics* 49, 1236 1243 (2010)
- [27] Herrera, L., Santos, N.: Jeans mass for anisotropic matter. *The Astrophysical Journal* 438, 308 313 (1995)
- [28] Herrera, L., Santos, N.O.: Local anisotropy in self-gravitating systems. *Physics Reports* 286(2), 53 130 (1997)
- [29] Herrera, L., Santos, N.: Thermal evolution of compact objects and relaxation time. *Monthly Notices of the Royal Astronomical Society* 287(1), 161 164 (1997)
- [30] Mak, M., Harko, T.: New method for generating general solution of abel differential equation. *Computers & Mathematics with applications* 43(1-2), 91 94 (2002)

- [31] Mak, M., Harko, T.: An exact anisotropic quark star model. Chinese journal of astronomy and astrophysics 2(3), 248 (2002)
- [32] Chan, R., Da Silva, M., Rocha, J.F.V.: Gravitational collapse of self-similar and shear-free uid with heat ow. International Journal of Modern Physics D 12(03), 347 368 (2003)
- [33] Harko, T., Mak, M.: Anisotropy in bianchi-type brane cosmologies. Classical and Quantum Gravity 21(6), 1489 (2004)
- [34] G. Lema tre, Ann. Soc. Sci. Brux. A 53 (1933) 51.
- [35] R.L. Bowers, E.P.T. Liang, Astrophys. J. 188 (1974) 657.
- [36] P.S. Letelier, Phys. Rev. D 22 (1980) 807.
- [37] T. Harko, F.S.N. Lobo, Phys. Rev. D 83 (2011) 124051.
- [38] L. Herrera, J. Ospino, A. Di Prisco, Phys. Rev. D 77 (2008) 027502.
- [39] M. Sharif, S. Sadiq, Eur. Phys. J. C 78 (2018) 410.
- [40] K.N. Singh, S.K. Maurya, M.K. Jasim, F. Rahaman, Eur. Phys. J. C 79 (2019) 851.
- [41] B. P. Abbott, R. Abbott, T. D. Abbott, M. R. Abernathy, F. Acernese, K. Ackley, C. Adams, T. Adams, P. Addesso, R. X. Adhikari, and et al., Observation of Gravitational Waves from a Binary Black Hole Merger, Phys. Rev. Lett. 116, 061102 (2016).
- [42] C. Chirenti and L. Rezzolla, Did GW150914 produce a rotating gravastar?; arXiv:1602.08759 [gr-qc].
- [43] Malaver, M., Daei Kasmaei, H.: Relativistic stellar models with quadratic equation of state. International Journal of Mathematical Modelling & Computations 10(2 (SPRING)), 111 124 (202)
- [44] J Cottam, F Paerels, and Mendez, Nature 420(6911), 51-54 (2002)
- [45] F zel, Nature 441(7097),1115-1117 (2006)
- [46] H Rodrigues, S Duarte, and J Oliveira, The Astrophysical Journal 730(1), 31 (2011)
- [47] B Ivanov, Physical Review D 65(10), 104001 (2002)
- [48] R Sharma and S Maharaj, Monthly Notices of the Royal Astronomical Society 375(4), 1265-1268 (2007)

- [49] S Thirukkanesh and F Ragel, *Pramana J. Phys.* 83 (275), (83-93) (2013)
- [50] S Thirukkanesh and S Maharaj, *Classical and Quantum Gravity* 25(23), 235001 (2008)
- [51] V Varela, F Rahaman, S Ray, K Chakraborty, and M Kalam, *Physical Review D* 82(4), 044052 (2010)
- [52] K Komathiraj and S D Maharaj, *International Journal of Modern Physics D* 16(11), 1803-1811 (2007)
- [53] M K Mak and T. Harko, *Chinese journal of astronomy and astrophysics* 2(3), 248 (2002)
- [54] M. Mannarelli, F. Tonelli, Gravitational wave echoes from strange stars *Phys. Rev. D* 97, 123010 (2018)
- [55] P. Pani, V. Ferrari, On gravitational-wave echoes from neutron-star binary coalescences, *Class. Quan. Grav.* 35, 15LT01 (2018)
- [56] Bora, J., Dev Goswami, U. (2022). Gravitational Wave Echoes from Strange Stars for Various Equations of State. In: Mohanty, B., Swain, S.K., Singh, R., Kashyap, V.K.S. (eds) *Proceedings of the XXIV DAE-BRNS High Energy Physics Symposium, Jatni, India. Springer Proceedings in Physics*, vol 277. Springer, Singapore. https://doi.org/10.1007/978-981-19-2354-8_122
- [57] [57] M Cosenza, L Herrera, M Esculpi and L Witten, *Journal of Mathematical Physics* 22(1), 118-125 (1981)
- [58] S Maharaj, J Sunzu and S Ray, *The European Physical Journal Plus* 129, 1-10 (2014)
- [59] F Weber, *Prog. Part. Nucl. Phys* 54, 193 (2005)
- [60] Mafa Takisa and S. D. Maharaj, *Astrophysics and Space Science* 343, 569-577(2013)
- [61] H Sotani, K. Kohri and T. Harada, *Phys. Rev. D* 69, 084008 (2004)
- [62] J M Sunzu and P. Danford, *Pramana J. Phys.* 89, 44 (2017)
- [63] Patel, R., & Ratanpal, B.S. (2023). A various equation of state for anisotropic models of compact star.
- [64] Nasheeha, R.N., Thirukkanesh, S. & Ragel, F.C. Anisotropic models for compact star with various equation of state. *Eur. Phys. J. Plus* 136, 132 (2021). <https://doi.org/10.1140/epjp/s13360-021-01118-3>

- [65] A class of relativistic stars with a linear equation of state R. Sharma, S. D. Maharaj Monthly Notices of the Royal Astronomical Society, Volume 375, Issue 4, March 2007, Pages 1265-1268, <https://doi.org/10.1111/j.1365-2966.2006.11355.x>
- [66] Charged anisotropic matter with a linear equation of state S Thirukkanesh and S D Maharaj Published 12 November 2008 2008 IOP Publishing Ltd Classical and Quantum Gravity, Volume 25, Number 23 Citation S Thirukkanesh and S D Maharaj 2008 Class. Quantum Grav. 25 235001 DOI 10.1088/0264-9381/25/23/235001
- [67] E Babichev¹, V Dokuchaev¹ and Yu Eroshenko¹ Published 7 December 2004 2005 IOP Publishing Ltd Classical and Quantum Gravity, Volume 22, Number 1 Citation E Babichev et al 2005 Class. Quantum Grav. 22 143 DOI 10.1088/0264-9381/22/1/010
- [68] M Esculpi and E Aloma, The European Physical Journal C 67, 521-532 (2010)
- [69] Nilsson et al, General Relativistic Stars: Linear Equations of State February 2000 Annals of Physics 286(2):278-291 DOI:10.1006/aphy.2000.6089
- [70] K Pant and P Fuloria, New Astron., 84, 101509 (2021)
- [71] R.C. Tolman, Phys. Rev. 55 (1939) 364
- [72] Oppenheimer J.R., Volk G.M., Phys. Rev. 55 (1939) 374.
- [73] L Herrera and N O Santosh, Phys. Rep. 286, 53-130 (1997)
- [74] H Abreu, H Hernandez and L A N ez, Class. Quantum Grav. 24, 4631 (2007)
- [75] R. C. Tolman, Phys. Rev. 55 (1939) 364, <https://link.aps.org/doi/10.1103/PhysRev.55.364>
- [76] S. Biswas⁷¹, D. Shee, B. K. Guha and S. Ray, Eur. Phys. J. C 80 (2020) 175 <https://doi.org/10.1140/epjc/s10052-020-7725-0>.
- [77] P. Bhar, K. N. Singh and F. Tello-Ortiz, Eur. Phys. J. C 79 (2019) 922, <https://doi.org/10.1140/epjc/s10052-019-7438-4>.
- [78] Piyali Bhar, Shyam Das, and Bikram Keshari Parida International Journal of Geometric Methods in Modern Physics Vol. 19, No. 06, 2250095 (2022)
- [79] T Gangopadhyay, S Ray, X-D Li, J Dey and M Dey, 512 Mon. Not. R. Astron. Soc. 431, 3216 (2013)